Conformational Analysis of Broken Rodlike Chains. 2. Conformational Analysis of Poly(D-glutamic acid) in Aqueous Solution by Small-Angle X-ray Scattering

Yoshio Muroga*

Faculty of Engineering, Nagoya University, Chikusa-ku, Nagoya 464, Japan

Hiroyuki Tagawa

Faculty of Science and Technology, Nihon University, Chiyoda-ku, Tokyo 101, Japan

Yuzuru Hiragi

Institute for Chemical Research, Kyoto University, Uji, Kyoto 611, Japan

Tatzuo Ueki

Faculty of Engineering Science, Osaka University, Toyonaka, Osaka 560, Japan

Mikio Kataoka

Faculty of Science, Tohoku University, Sendai, Miyagi 980, Japan

Yoshinobu Izumi

Faculty of Science, Hokkaido University, Sapporo, Hokkaido 060, Japan

Yoshiyuki Amemiya

National Laboratory for High Energy Physics, Oho-machi, Tsukuba-gun, Ibaragi 305, Japan. *Received November 20, 1987; Revised Manuscript Received February 22, 1988*

ABSTRACT: The conformations of poly(D-glutamic acid), PDGA, in helix, helix-to-coil transition, and random coil regions were studied by small-angle X-ray scattering. Analysis of data was carried out by comparing the observed scattering curves with theoretical ones for broken rods, rodlike chains joined by flexible coils, and random coils, respectively, as presented in the preceding paper in this issue. It is shown that the conformation of helical PDGA can be represented by freely hinged rods each of length of ca. 45 Å, whereas the conformation in the helix-to-coil transition region can well be represented by a model of several rods joined by flexible coils. The scattering curve of the random-coiled form is far from the Debye function.

Introduction

Ever since the conformational transition of poly(D- or L-glutamic acid) (PGA) was discovered by Doty et al.,[1,2] PGA has attracted great interest[3-6] as a model for the formation of protein structures because of the existence of α-helical regions in natural proteins. As a result, the local and overall conformations of PGA in the helical region, the helix-to-coil transition region, and the randomly coiled region have been well characterized. However, details on the conformation during the helix-to-coil transition still remain unclear. That is, the molecule in a helix-to-coil transition region is supposed to consist of a mixture of helical rods and random coils, but the detail in the mixture has not yet been clarified. Moreover, the detail in the structure of the molecule in a helical region has not been made clear either.

In the preceding paper in this issue,[7] it was pointed out that such conformations of polypeptides, which usually have broad molecular weight distributions, could be clearly resolved if we observe the particle-scattering function in the range of large wave vector, h, in small-angle X-ray scattering (SAXS). In the large h range of X-ray scattering, the particle-scattering function is insensitive to molecular weight and also molecular weight distribution, since the scattering from only a part of the chain can be observed. In the present work, the conformations of PGA in three conformational regions are analyzed by SAXS. The conformational analysis is carried out through comparison of observed scattering curves with corresponding theoretical ones, derived in the preceding paper[7] in this issue.

Table I
Three Samples for SAXS Measurements

	samples	C_p, g/dL	i	C_s, N
(PDGA)	A	0.53	0.275	0.02
	B	0.53	0.500	0.02
	C	0.53	0.900	0.10

Experimental Section

(1) Samples and Preparation. Poly(D-glutamic acid), PDGA, kindly provided by Ajinomoto Inc., was purified by precipitation from aqueous solution with a 1:3 mixture of methanol and acetone and, after dialyzation, was freeze-dried from aqueous solution. The apparent number-averaged (3.3×10^4) and apparent weight-averaged molecular weights (5.5×10^4) were determined by gel permeation chromatography (Toyo Soda GPC HLC-802A), using a coiled state of the sample with degree of neutralization of 100% in 0.3 N NaCl and poly(ethylene glycol) as a standard sample.

Three samples of PDGA (sample A, B, and C) were prepared for the measurements of SAXS. According to the potentiometric titration method, the degree of neutralization (i) was adjusted to preassigned values so that the sample may take different conformations: helix (rod) form (sample A), a mixture of helix and coil forms (B), and a random-coiled form (C). The helix content of sample B was 56% from the analysis of the potentiometric titration curve.[4] The values of i and an added salt concentration, C_s, for three samples are listed in Table I. The polymer concentrations (C_p) of all samples were fixed to be 0.53 g/dL.

0024-9297/88/2221-2756$01.50/0

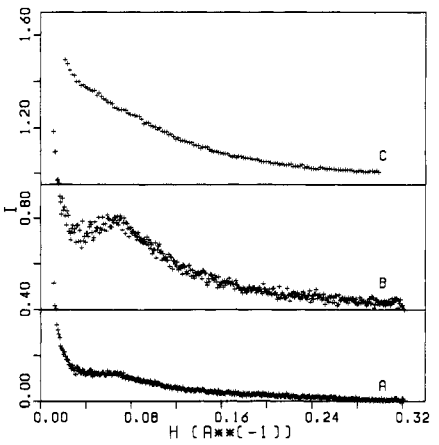

Figure 1. Observed scattering curves of poly(sodium D-glutamate), PDGA, with various degrees of neutralization, i, and added salt concentrations, Cs: A, sample A, i = 0.275, Cs = 0.02 N; B, sample B, i = 0.500, Cs = 0.02 N; C, sample C, i = 0.900, Cs = 0.10 N. Polymer concentration, C_p, is 0.53 g/dL for all samples. Curves B and C were shifted a distance of 0.40 and 0.95 upward along the ordinate, respectively.

(2) Measurements of SAXS. In order to get a sufficiently high signal-to-noise ratio from such a dilute solution of PDGA (C_p = 0.53 g/dL), the SAXS experiments were carried out on a focusing optics using synchrotron radiation as an X-ray source, set up in the Photon Factory of the National Laboratory for High Energy Physics at Tsukuba, Japan. The wavelength of the X-ray was 1.488 Å, and the distance between the sample and the plane of registration was 1900 mm. The scattering intensity was detected by a position-sensitive proportional counter (PSPC) with 512 channels. The details of the instrumentation and the procedure are described elsewhere.[8]

The scattering intensities recorded were not converted to those on an absolute scale. Therefore, observed scattering intensities were allowed to be multiplied by a suitable factor for fitting to a theoretical curve.

(3) Numerical Computations. The data analysis of PDGA was carried out according to the following process. The net scattering intensities from solute molecules, I_{obs}, which were given as the difference between the observed scattering intensities for solutions and solvents, were analyzed without any slit corrections, since the size of the X-ray source was small enough to be able to regard it as a pinhole source.

For a thick molecule, I_{obs} is a product of I_{thin} and I_{cs},[9,10] where I_{thin} is the scattering intensity from a hypothetical polymer coil with zero cross section and I_{cs} is the scattering intensity from a cross section of a polymer coil. Needless to say, I_{thin} can be compared with theoretical scattering curves, which are, in general, developed for a hypothetical polymer chain with no cross section.

I_{cs} is theoretically expressed by[10]

$$I_{cs} \propto \exp\{-(1/2)\langle R_{cs}^2\rangle h^2\} \quad (1)$$

where $\langle R_{cs}^2\rangle^{1/2}$ is the radius of gyration of the cross section, and h is the magnitude of the wave vector, defined by $(4\pi/\lambda)\sin(\theta/2)$, where θ is the scattering angle, and λ is the wavelength of the incident beam (1.488 Å). As is well-known, I_{thin} of a rod molecule is inversely proportional to h,[9,10] so the plot of ln $(I_{obs}h)$ vs h^2 should be a straight line, according to eq 1. From its slope we can estimate the values of $\langle R_{cs}^2\rangle$. A polymer coil can be regarded as a rod molecule in a following scattering angle range:

$$1/L < h < 1/\langle R_{cs}^2\rangle^{1/2} \quad (2)$$

where L denotes the length of a rod. If the above procedure is applied to the data in the scattering angle range given by eq 2, the values of $\langle R_{cs}^2\rangle$ for PGA and then I_{cs} can be evaluated. I_{thin} can be calculated from the experimental data of I_{obs} and I_{cs} thus obtained and then employed in the plot of $I_{thin}h^2$ vs h.

Results

Figure 1 shows the observed scattering curves of PDGA, I_{obs}, vs h. This scattering behavior is the one characteristic

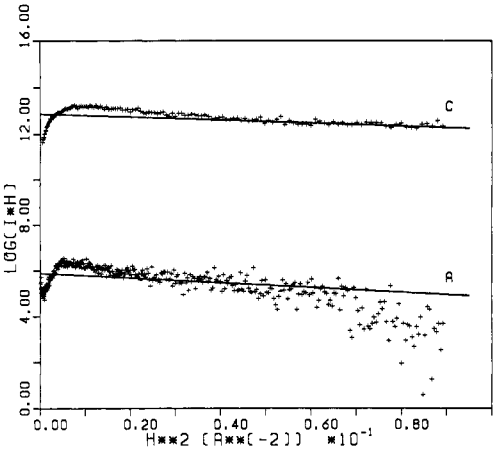

Figure 2. Plot of ln $(I_{obs}h)$ vs h^2 for estimating the radius of gyration of cross section of PDGA chain: A, sample A; C, sample C.

of ordinary polyelectrolyte solutions:[11-18] a maximum appears in the range of h of about 0.06–0.07 Å^{-1}, and it is accentuated and moves to a higher angle, as i becomes higher. The maximum may be due to a combination of intra- and intermolecular interferences as was proved in a small-angle neutron-scattering experiment.[16] Therefore, discussion in the present paper should be given to the data above ca. 0.08 Å^{-1} in h.

Since sample A takes a helix form, its conformation can be regarded as a rod. Sample C, which has a randomly coiled conformation, is also regarded as a rod if observations are done at sufficiently high angles to satisfy eq 2. In these rod regions, the effect of cross section on scattering curve can be estimated from the plot of ln $(I_{obs}h)$ vs h^2, as stated in the Experimental Section. As shown in Figure 2, the plots can be regarded as straight lines with negative slopes in the range of h^2 of 0.022–0.054 Å^{-2} for sample A and 0.040–0.088 Å^{-2} for sample C. From the slopes, we can estimate the radii of gyration of cross section, $\langle R_{cs}^2\rangle^{1/2}$, to be 4.3 and 1.1 Å for samples A and C, respectively. It is clear that the products of these values and corresponding upper scattering angle limit, $0.054^{1/2}$ and $0.088^{1/2}$ Å^{-1}, respectively, are smaller than unity, obeying eq 2.

The conformation of sample B takes a mixture of helix and coiled forms, and hence, the above procedure for the estimation of the radius of gyration of cross section, $\langle R_{cs}^2\rangle_B$, cannot be applied to this sample. However, it can be shown[19] that $\langle R_{cs}^2\rangle_B$ may be calculated from $\langle R_{cs}^2\rangle_{helix}$ for the helical form and from $\langle R_{cs}^2\rangle_{coil}$ for the coiled form, according to the following relation:

$$\langle R_{cs}^2\rangle_B = g\langle R_{cs}^2\rangle_{helix} + (1-g)\langle R_{cs}^2\rangle_{coil} \quad (3)$$

if the helix content g is known. If the observed helix content of sample B, g = 0.56, and $\langle R_{cs}^2\rangle$ for sample A and C, corresponding to $\langle R_{cs}^2\rangle_{helix}$ and $\langle R_{cs}^2\rangle_{coil}$, respectively, are substituted into eq 3, $\langle R_{cs}^2\rangle_B^{1/2}$ can be estimated to be 3.3 Å.

From these values of $\langle R_{cs}^2\rangle$, we can calculate I_{cs} and, consequently, I_{thin} for the three samples. I_{thin} thus obtained was plotted in the form of $I_{thin}h^2$ vs h in Figure 3.

Discussion

The conformations of PDGA in the helical region, the helix-to-coil transition region, and the randomly coiled region may be represented by freely hinged rod, rodlike chain joined by flexible coils, and randomly coiled chain, respectively. As shown in the preceding paper[7] in this

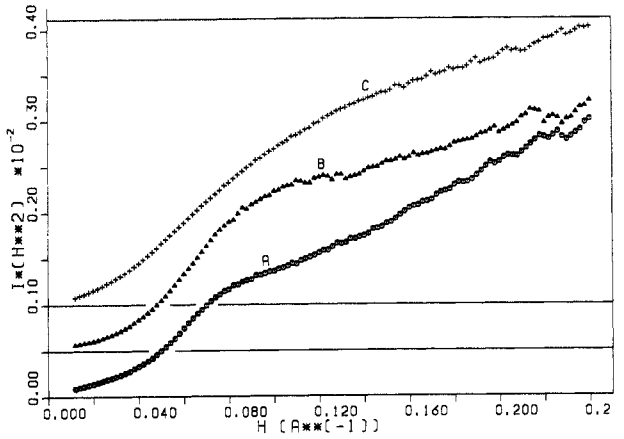

Figure 3. Observed Kratky plot, $I_{thin}h^2$ vs h, for PDGA: A, sample A; B, sample B; C, sample C. Curves B and C were shifted a distance of 0.05×10^{-2} and 0.1×10^{-2} upward along the ordinate, respectively.

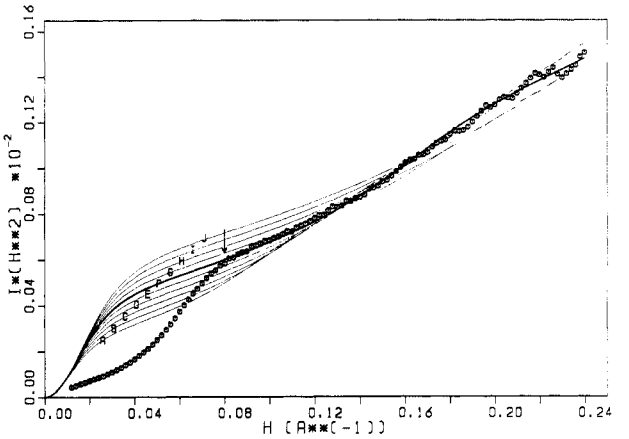

Figure 4. Comparison between the observed Kratky plot, $I_{thin}h^2$ vs h, of sample A (open circles) and the calculated ones for freely hinged rods of various numbers, N_0: A, 7; B, 8; C, 9; D, 10; E, 11; F, 12; G, 13; H, 14; I, 15; J, 16. The contour length of the polymer chain L = 1315 Å. An arrow in the figure indicates the value of h, above which the normalized particle-scattering function becomes insensitive to the molecular weight.

issue, the reduced scattering intensities for all these models are given by the following equation:

$$\frac{\langle R_\theta \rangle}{(NA + Nna)^2} = \frac{f^2}{N}\left\{2\Lambda(\beta) - \frac{4}{\beta^2}\sin^2\frac{\beta}{2}\right\} + \frac{2f^2}{N}\Lambda^2(\beta)\left(\frac{e^{-w}}{1-\nu e^{-w}}\right) - \frac{2f^2}{N^2}\Lambda^2(\beta)\left(\frac{e^{-w}}{1-\nu e^{-w}}\right)\left(\frac{1-(\nu e^{-w})^N}{1-\nu e^{-w}}\right) + (1-f)^2\left\{\frac{2}{Nw} - 2\left(\frac{1-e^{-w}}{Nw}\right)^2\left(\frac{\nu}{1-\nu e^{-w}}\right)\left(\frac{1-(\nu e^{-w})^N}{1-\nu e^{-w}}\right) - 2\frac{(1-e^{-w})(1-\nu)}{Nw^2(1-\nu e^{-w})}\right\} + \frac{2f(1-f)}{N^2}\frac{\Lambda(\beta)(1-e^{-w})}{w(1-\nu e^{-w})}\left\{2N - \frac{(1+\nu e^{-w})(1-(\nu e^{-w})^N}{1-\nu e^{-w}}\right\} \quad (4)$$

where f is the ratio of contour length of rod portions to that of a whole polymer chain, such as

$$f = \frac{NA}{nNa + NA} \quad (5)$$

w, $\Lambda(\beta)$, β, and ν are defined by the following equations:

$$w = \frac{n\alpha^2}{6} = \frac{na^2}{6}\left(\frac{4\pi}{\lambda}\right)^2 \sin^2\left(\frac{\theta}{2}\right) \quad (6)$$

$$\Lambda(\beta) = (1/\beta)\int_0^\beta (\sin t/t)\, dt \quad (7)$$

$$\beta = Ah \quad (8)$$

$$\nu = \frac{\sin\beta}{\beta} \quad (9)$$

In general, eq 4 represents the scattering intensity for N rods of length A joined alternatively by N random coils, each of which consists of n segments of length a. In the extreme cases of $f = 0$ and $f = 1$, it represents ones for random coil chain and freely hinged rods, respectively.

In the sample preparation, we usually express the helix content g by the ratio of the number of monomers involved in rod portions to that in the whole polymer chain.

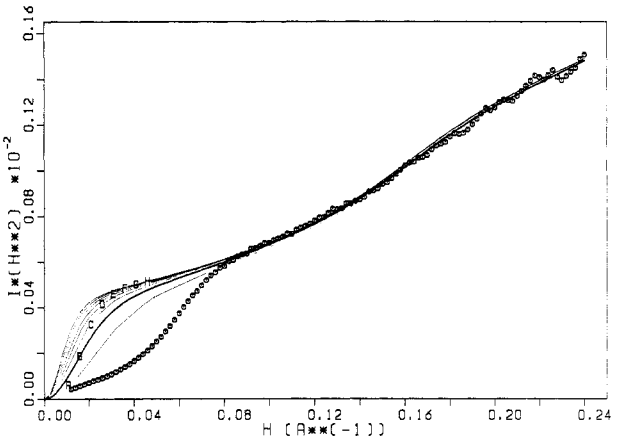

Figure 5. Comparison between the observed Kratky plot, $I_{thin}h^2$ vs h, of sample A (open circles) and the normalized theoretical ones for freely hinged rods of various contour lengths, L: A, 658; B, 1315; C, 1973; D, 2630; E, 3290; F, 3948; G, 4606; H, 5260 Å. The rod length A_0 = 45 Å.

Therefore, it seems more practical to express eq 4 in terms of helix content, g. The helix content, g, is given by

$$g = \frac{cNA}{nNa + cNA} \quad (10)$$

Since f is related to g through the relation,

$$f = \left\{1 + c\left(\frac{1}{g} - 1\right)\right\}^{-1} \quad (11)$$

the reduced scattering intensity in eq 4 can be regarded as a function of g. In the case of PDGA, c is estimated to be 2.41 on the basis of molecular data that the pitch of the helical PDGA is 5.4 Å/turn and its 5 turns involve 18 monomer units and the length of 1 monomer unit is 3.615 Å.[20]

The observed scattering curve of sample A was analyzed by comparing it with the theoretical curve for broken rods, eq 29 in the preceding paper,[7] which can be obtained from eq 4 with $f = 1$. In theory, an unknown parameter, the number of broken rods in the molecule (N_0), or its length (A_0) is required for calculation if the contour length of the polymer chain at the unhelical state (L) is given. That is, we have the following relationship:

$$L = cN_0A_0 \quad (12)$$

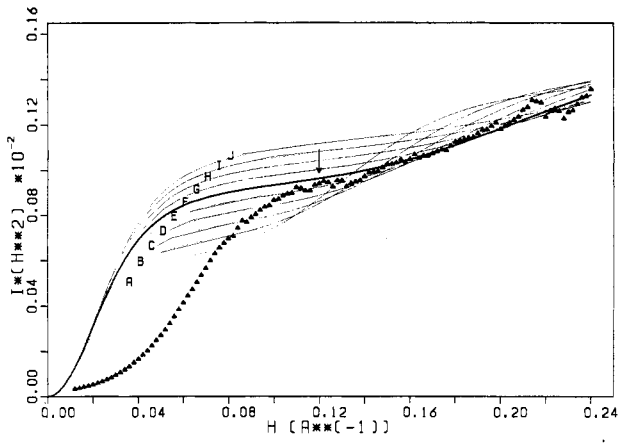

Figure 6. Comparison between the observed Kratky plot, $I_{thin}h^2$ vs h, of sample B (filled triangles) and the calculated ones for broken rods joined by flexible coils with various rod numbers, N_0: A, 7; B, 8; C, 9; D, 10; E, 11; F, 12; G, 13; H, 14; I, 15; J, 16. The contour length of polymer chain L = 1315 Å and the coil length a = 8 Å. An arrow in the figure has the same meaning as in Figure 4.

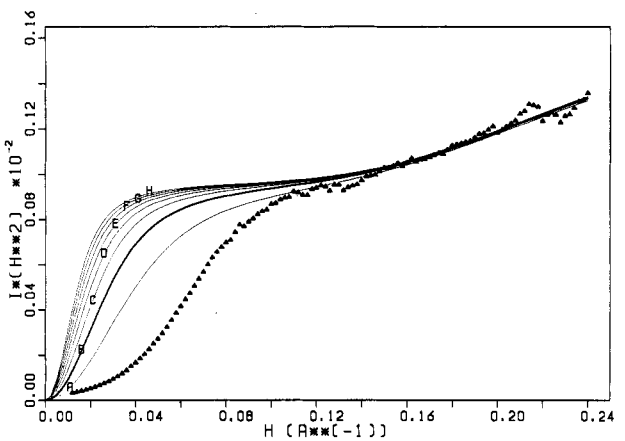

Figure 7. Comparison between the observed Kratky plot, $I_{thin}h^2$ vs h, of sample B (filled triangles) and the normalized theoretical ones for broken rods joined by flexible coils with various contour lengths: A, 658; B, 1315; C, 1973; D, 2630; E, 3290; F, 3948; G, 4606; H, 5260 Å. The rod length A = 25 Å and the coil length a = 8 Å.

The molecular weight of PDGA per unit contour length is 41.8 Å^{-1}, and the weight-averaged molecular weight of the present sample is 5.5×10^4, so L is estimated to be ca. 1315 Å. If we fix L, therefore, calculated scattering curves are obtained as a function of N_0. The calculated curves are shown, together with the observed one of sample A, in Figure 4.

As easily seen, the observed scattering curve can be satisfactorily reproduced by a theoretical curve with N_0 of 12, except in a lower scattering angle region of less than 0.08 Å^{-1}, where the observed scattering curve should also be contaminated by possible intermolecular interactions, judging from the appearance of a bump in Figure 1. If N_0 thus obtained is substituted into eq 12, A_0 can be estimated to be ca. 45 Å. Since the normalized theoretical scattering curves, obtained by multiplying the intensities by the contour length of a chain, are almost independent of the contour length above 0.08 Å^{-1}, as seen in Figure 5, the value of A_0 seems to be unaltered even when the molecular weight distribution of PDGA is taken into consideration. A_0 thus obtained satisfies the relation given by eq 2: the product of A_0 and the observed lower limit in Figure 2, $0.022^{1/2}$ Å^{-1}, are sufficiently larger than unity.

The observed scattering curve of sample B was analyzed through comparison with theoretical curves for broken rods joined by flexible coil portions, eq 4. In eq 4, we need to know the three values of N, A, and w, which is a function of the number of segments in a coil portion n, segment length a, and scattering angle θ, as shown by eq 6. However, we have the following interrelations among N, A, n, and a:

$$L = nNa + cNA \tag{13}$$

in addition to eq 6 and 10. Here, it is assumed that the length of a is equal to the unperturbed effective bond length of randomly coiled PGA, 8 Å, which was obtained from the measurements of the light scattering and the intrinsic viscosity by Hawkins and Holtzer.[21] Under this assumption, A and Rg^2 can be expressed as a function of N, where Rg^2 is defined as $na^2/6$ so that it can be related to w through the relation, $w = Rg^2h^2$. The calculated scattering curves are shown as a function of N, together with the observed curve of sample B, in Figure 6.

It is evident that the observed scattering curve of sample B is in good agreement with a theoretical one with N = 12, the same number for sample A, except in a lower scattering angle region. The reason for the disagreement in the low-angle region would be the same as in the case of sample A. From the fact that normalized theoretical scattering curves with various contour lengths are almost coincident above 0.12 Å^{-1}, as seen in Figure 7, it seems certain that the value of N thus determined is not altered by taking into account the molecular weight distribution of the sample. The coincidence of the breaking points, N (=12), in PDGA in a helical region and in a helix-to-coil transition region seems to suggest that helix-to-coil transition of PDGA might proceed by extending a region of disordered portions at hinges of the helical rods.

It is of interest to compare our present result with that obtained from the analysis of the helix–coil transition curve on the basis of the statistical theories.[22] According to these theories, the average number of residues per helical sequence, n_N, in a sufficiently long chain at the midpoint of the helix–coil transition can be related to the initiation parameter for the formation of helical sequences, σ, as follows:

$$n_N = \sigma^{-1/2} \tag{14}$$

Snipp et al. report that $\sigma = 3 \pm 2 \times 10^{-3}$ for poly(L-glutamic acid) in aqueous solution.[23] Using $\sigma = 3 \times 10^{-3}$, we can obtain n_N = 18. This value is in satisfactory agreement with our present result of n_N = 17 at the helical content of 0.56.

The observed scattering curve of sample C was analyzed through comparison with theoretical curves for random coils, eq 27 in the preceding paper.[7] The length, a, was assumed to be 8 Å. In Figure 8 are shown the normalized theoretical scattering curves as a function of contour length, together with an observed curve of sample C. It is clear that the scattering curve of sample C cannot be represented by that of a Gaussian chain. The reason for this discrepancy may be the same as observed for flexible polyelectrolytes, poly(sodium acrylate).[24,25] That is, the segment distribution in the polyelectrolyte coil is far from the Gaussian distribution. In the calculation for sample B, too, it is assumed that the Debye model is applicable to coiled portions in the sample. In this case, however, the failure of the Debye model does not manifest itself, probably since the contribution of the coiled portion to the whole Ih^2 vs h curve is smaller.

Equation 4 has been derived for an ideal single chain. Accordingly, it is required that eq 4 should be applied to an isolated chain in solution. That is, the concentration

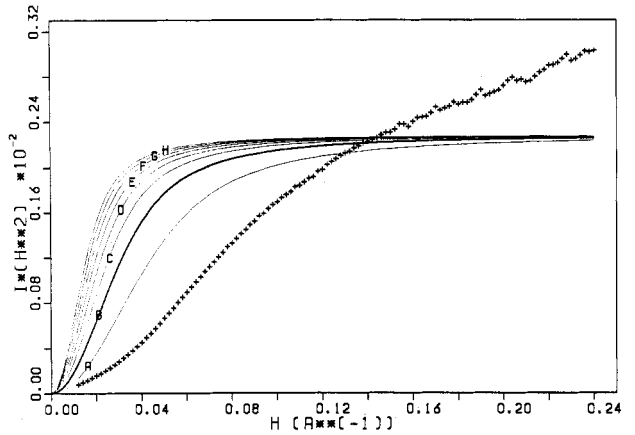

Figure 8. Comparison between the observed Kratky plot of sample C (crosses) and the normalized theoretical ones for a Gaussian chain with various contour lengths: A, 658; B, 1315; C, 1973; D, 2630; E, 3290; F, 3948; G, 4606; H, 5260 Å. The coil length a = 8 Å.

of sample solutions should be dilute enough compared with a critical concentration, C_p^*, where polymer chains are set to overlap one another. C_p^* in grams/milliliter is given by

$$C_p^* = \frac{M_w}{A_v(4/3)\pi\langle S^2\rangle^{3/2}10^{-24}} \quad (15)$$

where M_w, A_v, and $\langle S^2\rangle^{1/2}$ are the molecular weight, Avogadro's number, and the radius of gyration of a polymer chain in angstroms, respectively. If the values of a, L, and A_0 obtained above are employed, C_p^*'s for samples A and C are roughly estimated to be 6.8 and 12.0 g/dL, respectively. The present sample concentration, 0.53 g/dL, is sufficiently smaller then these values of C_p^*.

Finally, it should be added that it is not clear from this work whether 45 Å obtained for each length of freely hinged rods is a physical constant for a helical PGA or not. More experiments using the samples with different molecular weights may be required to answer the question.

Acknowledgment. We are indebted to Professor M. Nagasawa of Toyota Technological Institute for valuable discussions and critical reading of the manuscript and also to Professor M. Nagura of Shinshu University for helping us with the SAXS experiments.

Registry No. PDGA (homopolymer), 25104-13-6; PDGA (SRU), 27030-24-6.

References and Notes

(1) Doty, P.; Wada, A.; Yang, J. T.; Blout, E. R. *J. Polym. Sci.* **1957**, *23*, 851.
(2) Wada, A. *J. Mol. Phys.* **1960**, *3*, 409.
(3) Zimm, B. H.; Rice, S. A. *J. Mol. Phys.* **1960**, *3*, 391.
(4) Nagasawa, M.; Holtzer, A. *J. Am. Chem. Soc.* **1964**, *86*, 538.
(5) Muroga, Y.; Suzuki, K.; Kawaguchi, Y.; Nagasawa M. *Biopolymers* **1972**, *11*, 137.
(6) Olander, D.; Holtzer, A. *J. Am. Chem. Soc.* **1968**, *90*, 4549.
(7) Muroga, Y. *Macromolecules* **1988**, *21*, preceding paper in this issue.
(8) Ueki, T.; Hiragi, Y.; Izumi, Y.; Tagawa, H.; Kataoka, M.; Muroga, Y.; Matsushita, T.; Amemiya, Y. *Photon Factory Activity Rep.* 1982–1983, *6*, 70.
(9) Kratky, O.; Porod, G. *Acta Phys. Aust.* **1948**, *2*, 133.
(10) Porod, G. *Acta Phys. Aust.* **1948**, 2, 255.
(11) Cotton, J. P.; Moan, M. *J. Phys. Lett.* **1976**, *37*, L75.
(12) Moan, M.; Wolff, C.; Cotton, J. P.; Ober, R. *J. Polym. Sci., Polym. Symp.* **1977**, *61*, 1.
(13) Moan, M. *J. Appl. Crystallogr.* **1978**, *11*, 519.
(14) Nierlich, M.; Williams, C. E.; Boue, F.; Cotton, J. P.; Daoud, M.; Farnoux, M.; Jannink, G. *J. Appl. Crystallogr.* **1978**, *11*, 504.
(15) Nierlich, M.; Williams, C. E.; Boue, F.; Cotton, J. P.; Daoud, M.; Farnoux, M.; Jannink, G.; Picot, C.; Moan, M.; Wolff, C.; Rinauld, M.; de Gennes, P. G. *J. Phys. Lett.* **1979**, *40*, 701.
(16) Williams, C. E.; Nierlich, M.; Cotton, J. P.; Jannink, G.; Boue, F.; Daoud, M.; Farnoux, M.; Picott, C.; de Gennes, P. G.; Rinaudo, M.; Moan, M.; Wolff, C. *J. Polym. Sci., Polym. Lett. Ed.* **1979**, *17*, 379.
(17) Ise, N.; Okubo, T.; Hiragi, Y.; Kawai, H.; Hashimoto, T.; Fujimura, M.; Nakajima, A.; Hayashi, H. *J. Am. Chem. Soc.* **1979**, *101*, 5836.
(18) Ise, N.; Okubo, T.; Yamamoto, K.; Kawai, H.; Hashimoto, T.; Fujimura, M.; Hiragi, Y. *J. Am. Chem. Soc.* **1980**, *102*, 7901.
(19) Kratky, O. In *Progress in Biophysics and Molecular Biology*; Butler, J. A. V., Huxley, H. E., Zirkle, R. E., Eds.; Pergamon: Oxford, 1963; Vol. 13, Chapter 3, pp 105–173.
(20) Walton, A. G. *Polypeptide and Protein Structure*; Elsevier–North Holland: Amsterdam, 1981; Chapters 1 and 2, pp 3–49.
(21) Hawkins, R. B.; Holtzer, A. *Macromolecules* **1972**, *5*, 294.
(22) Poland, D.; Scheraga, H. A. *Theory of Helix–Coil Transitions in Biopolymers*; Academic: New York, 1970.
(23) Snipp, R. L.; Miller, W. G.; Nylund, R. E. *J. Am. Chem. Soc.* **1965**, *87*, 3547.
(24) Kitano, T.; Taguchi, A.; Noda, I.; Nagasawa, M. *Macromolecules* **1980**, *13*, 57.
(25) Muroga, Y.; Noda, I.; Nagasawa, M. *Macromolecules* **1985**, *18*, 1576.